

# THE APOLLO 15 LUNAR HEAT-FLOW MEASUREMENT\*

MARCUS G. LANGSETH, JR.

*Lamont-Doherty Geological Observatory, Palisades, New York, U.S.A.*

SYDNEY P. CLARK, JR.

*Yale University, New Haven, Conn., U.S.A.*

JOHN L. CHUTE, JR. and STEPHEN J. KEIHM

*Lamont-Doherty Geological Observatory, Palisades, New York, U.S.A.*

and

ALFRED E. WECHSLER

*Arthur D. Little, Inc., Cambridge, Mass., U.S.A.*

**Abstract.** The heat-flow experiment is one of the Apollo Lunar Surface Experiment Package (ALSEP) instruments that was emplaced on the lunar surface on Apollo 15. This experiment is designed to make temperature and thermal property measurements in the lunar subsurface so as to determine the rate of heat loss from the lunar interior through the surface. About 45 days ( $1\frac{1}{2}$  lunations) of data has been analyzed in a preliminary way. This analysis indicates that the vertical heat flow through the regolith at one probe site is  $3.3 \times 10^{-6}$  W/cm<sup>2</sup> ( $\pm 15\%$ ). This value is approximately one-half the Earth's average heat flow. Further analysis of data over several lunations is required to demonstrate that this value is representative of the heat flow at the Hadley Rille site. The mean subsurface temperature at a depth of 1 m is approximately 252.4K at one probe site and 250.7K at the other. These temperatures are approximately 35K above the mean surface temperature and indicate that conductivity in the surficial layer of the Moon is highly temperature dependent. Between 1 and 1.5m, the rate of temperature increase as a function of depth is 1.75K/m ( $\pm 2\%$ ) at the probe 1 site. In situ measurements indicate that the thermal conductivity of the regolith increases with depth. Thermal-conductivity values between  $1.4 \times 10^{-4}$  and  $2.5 \times 10^{-4}$  W/cm K were determined; these values are a factor of 7 to 10 greater than the values of the surface conductivity. If the observed heat flow at Hadley Base is representative of the moonwide rate of heat loss (an assumption which is not fully justified at this time), it would imply that overall radioactive heat production in the Moon is greater than in classes of meteorites that have formed the basis of Earth and Moon bulk composition models in the past.

## 1. Experiment Concept and Design

The temperature and the heat flux at the surface of the Moon are determined mainly by the solar energy impinging on the surface during one-half of the 29.5-day lunation cycle. Between lunar dawn and lunar noon the surface temperature increases by nearly 300K. However, the extremely low thermal conductivity of the bulk of the regolith (Birkebak *et al.*, 1970) strongly inhibits the flow of heat into and out of the subsurface. At a depth of approximately 50 cm, the large variation of temperature at the surface during a lunation is attenuated to a nearly undetectable amplitude.

At depths greater than 50 cm, the thermal regime is dominated by heat flow from the lunar interior. This flow results from high interior temperatures and, in the sub-

\* Lamont-Doherty Geological Observatory Contribution Number 1800.

surface, is directly proportional to the increase of temperature with depth (the vertical temperature gradient,  $dT/dz$ ) and to the thermal conductivity,  $k$ . These quantities are related by the equation

$$F_z = -k \frac{dT}{dz}, \quad (1)$$

where  $F_z$  is the vertical component of the heat flow. The average heat flow of the Earth has been determined to be  $6.2 \times 10^{-6}$  W/cm<sup>2</sup> by numerous measurements (Lee *et al.*, 1965). Estimates of the lunar heat flow, based on microwave emission from the Moon, have ranged from  $1.0 \times 10^{-6}$  W/cm<sup>2</sup> (Baldin, 1961) to  $3.3 \times 10^{-6}$  W/cm<sup>2</sup> (Troitskiy and Tikhonova, 1970), or one-sixth to one-half the Earth heat flow. Thermal history calculations, based on chondritic and terrestrial isotope abundances for the Moon (see, for example, Fricker *et al.*, 1967), result in heat flow estimates of  $1 \times 10^{-6}$  to  $2.5 \times 10^{-6}$  W/cm<sup>2</sup> for the present time in the Moon's history. Because of the extremely low conductivity of the regolith, even these very low values of heat flow would result in gradients ranging from a few tenths of a degree per meter to a few degrees per meter.

## 2. Instrument Design

The essential measurements for determining heat flow are made by two slender temperature-sensing probes that are placed in predrilled holes in the regolith, spaced ap-

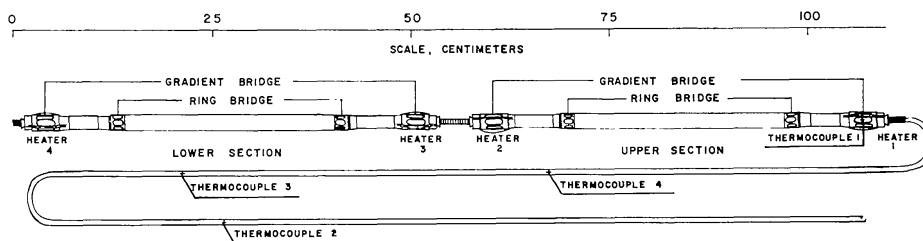


Fig. 1. Schematic of heat-flow probe.

proximately 10 m apart. Two probes enable two independent measurements of the heat flow to be made in order to gain some knowledge of the lateral variation of heat flow at the Hadley Rille site. Each probe consists of two nearly identical 50-cm-long sections (Figure 1). Each section of each heat flow probe has two accurate ( $\pm 0.001$  K) differential thermometers that measure temperature differences between points separated by approximately 47 and 28 cm. With these thermometers, measurements of absolute temperature with an accuracy of  $\pm 0.05$  K at four points on each probe section also can be made.

Additional temperature measurements are provided by four thermocouple junctions in the cables that connect each probe to the electronics unit. The thermocouple junctions are located at distances of approximately 0, 0.65, 1.15, and 1.65 m from the topmost gradient sensors (Figure 1). The reference junction for these thermocouples

TABLE I  
Summary of heat flow experiment temperature measurements

Thermometer	Number and location	Temperature difference		Absolute temperature	
		Range, K	Accuracy, K	Range, K	Accuracy, K
Gradient bridge <sup>a</sup>	1 per section, sensors separated by 47 cm	$\pm 2$ and $\pm 20$	$\pm 0.001$ and $\pm 0.01$	190 to 270	$\pm 0.05$
Ring bridge	1 per section, sensors separated by 28 cm	$\pm 2$	$\pm 0.002$	190 to 270	$\pm 0.05$
Thermocouple	4 per probe, in the first 2 m of the cable above probe	-	-	70 to 400	$\pm 0.7$
Thermocouple reference bridge	1 per experiment, mounted on radiation plate of electronics box	-	-	253 to 363	$\pm 0.01$

<sup>a</sup> Gradient bridge temperature difference measurements are made at two sensitivities with a ratio of 10 to 1.

is thermally joined to a platinum resistance reference thermometer, which is mounted on the radiator plate of the electronics unit. The temperature measurements obtained from the heat-flow experiment are summarized in Table I.

The differential thermometers consist of four platinum resistance elements wired in a bridge configuration (Figure 2a). The bridge is excited by successive 2.6-ms, 8-V pulses, first of one polarity and then of the other. The voltage output, excitation voltage, and bridge current are measured and used to determine absolute temperature and temperature difference. The ratio of bridge output voltage to excitation voltage and bridge resistance are calibrated at 42 different pairs of temperature and temperature difference values. The accuracy of these calibrations is better than the accuracies specified in Table I.

Conductivity measurements are made by means of heaters that surround each of the eight gradient-bridge sensors. The experiment is designed to measure conductivity in two ranges: a lower range of  $1 \times 10^{-5}$  to  $5 \times 10^{-4}$  W/cm-K and a higher range of  $2 \times 10^{-4}$  to  $4 \times 10^{-3}$  W/cm-K. To enable measurements in the lower range to be made, a heater is energized at 0.002 W, and the temperature rise of the underlying gradient sensor is recorded as a function of time for a period of 36 hr. The temperature rise and the rate of temperature rise can be interpreted in terms of the conductivity of the surrounding lunar material. Measurements in the higher range of conductivities are made by energizing the same heater at 0.5 W and monitoring the temperature rise at the ring sensor 10 cm away for a period of approximately 8 hr.

### 3. Operation of the Experiment

During normal operation of the experiment (mode 1 operation), temperatures of all gradient bridges, thermocouples, and the reference bridge (as well as temperature differences of all gradient bridges) are sampled every 7.2 min. When a heater is turned on at 0.002 W to enable measurements to be made in the lower conductivity range, the experiment is said to be operating in mode 2. The mode 3 operation is designed for the measurement of conductivity in the higher range. In this mode, temperature and temperature difference at a selected ring bridge are read every 54 s. These modes of operation and heater turn-on are controlled by commands transmitted from Earth.

The detection circuitry for measuring bridge voltages and thermocouple outputs is contained in a housing separate from the Apollo Lunar Surface Experiments Package (ALSEP) central station.

### 4. Emplacement of the Experiment at the Hadley Rille Site

Drilling of the holes to emplace the heat-flow probes was more difficult than had been expected. The resistant nature of the subsurface at the Hadley Rille site prevented penetration to the planned depth of 3 m. Instead, at the probe 1 site, the borestem penetrated 1.62 m; and, at the probe 2 site, the borestem penetrated approximately

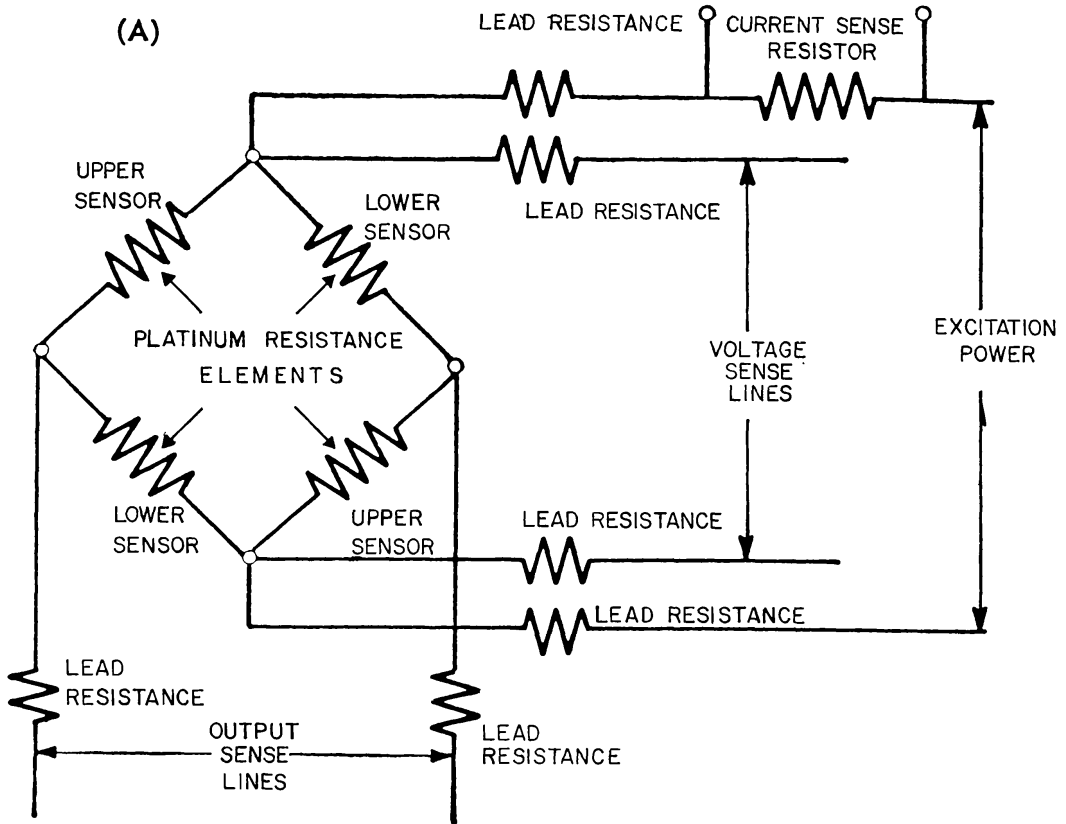


Fig. 2a.

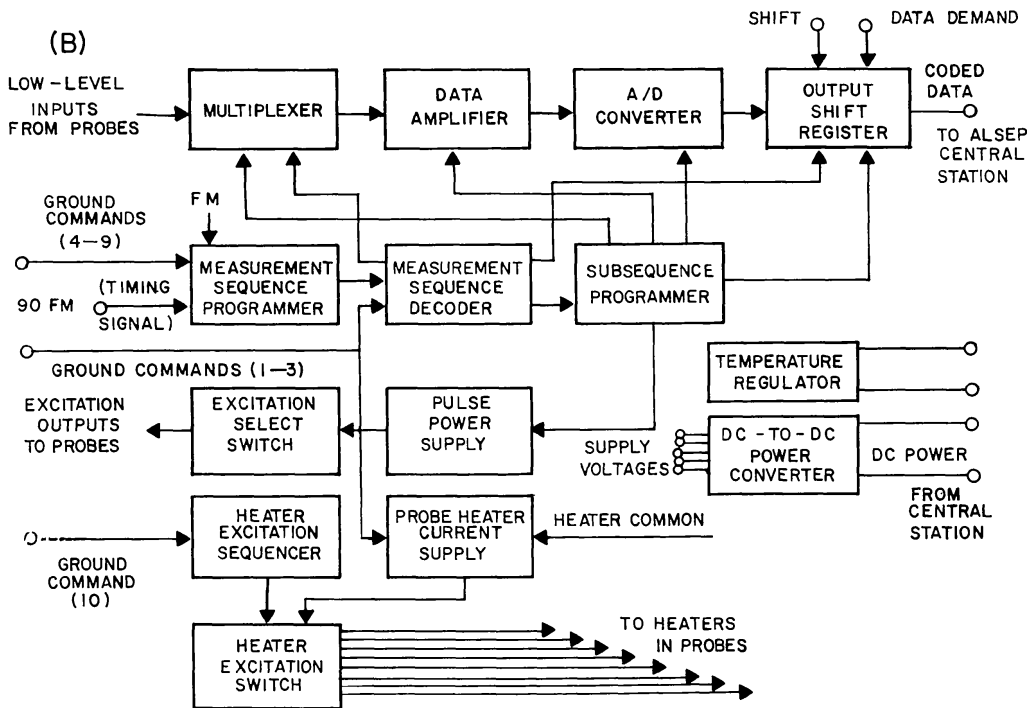


Fig. 2b.

Figs. 2a-b. Heat-flow experiment. (a) Circuit diagram of the differential thermometer. (b) Block diagram of the experiment electronics.

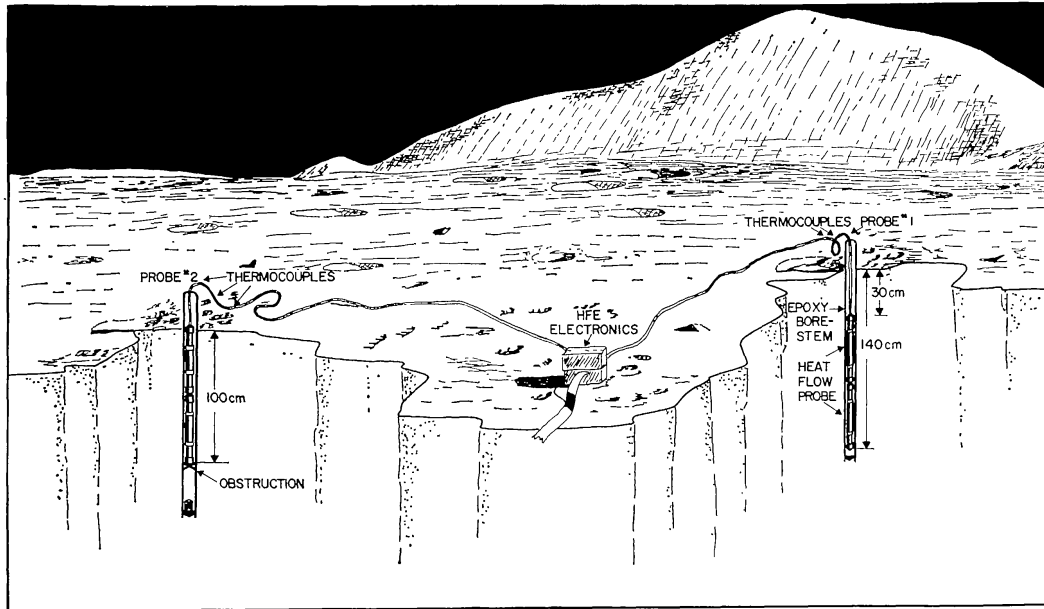


Fig. 3. A cutaway drawing of the heat-probe and thermocouple locations at the Hadley Rille site.

1.60 m. The configuration of the probe in each hole is shown in Figure 3. An obstruction, which was probably a break in the stem at a depth of approximately 1 m, prevented probe 2 from passing to the bottom of the borestem. Because of the very large temperature differences over the upper section, which extends above the surface, no valid temperature measurements were obtained by the ring and gradient bridges on the probe 2 upper section during most of the lunation cycle.

The shallow emplacement of the probes resulted in five of the cable thermocouples lying on, or just above, the lunar surface. These cable thermocouples come into radiative balance with the lunar surface and space, and the measured temperatures can be interpreted in terms of lunar-surface brightness temperatures. A sixth thermocouple is in the borestem projecting above the lunar surface at the probe 1 site.

### 5. Subsurface Temperatures

The surface-temperature measurements during the lunar night and during the August 6 eclipse indicate that the surface layer surrounding the probes has an extremely low thermal conductivity. The subsurface measurements, which will be discussed later in this paper, reveal that the conductivity increases substantially with depth, and values of approximately  $1.5 \times 10^{-4}$  W/cm-K are found at a depth of 1 m. With these values of conductivity, it is unlikely that any measurable time variation of temperature as a result of the diurnal cycle existed at depths below 50 cm before the borestem and the heat probe were emplaced. However, after emplacement, the relatively high thermal conductance of the borestem and the radiative transfer along the inside of the stem allowed surface-temperature variations to penetrate to greater depths. After several lunations, a new periodic steady-state condition will be established around the bore-

stem. Initially, however, the borestem and probes will equilibrate toward temperatures that existed in the subsurface before emplacement.

The temperature histories of all subsurface thermometers and the evolution of the profiles of temperature as a function of depth for probes 1 and 2 are shown in Figure 4 and 5, respectively. All sensors initially cooled very rapidly, and those sensors at

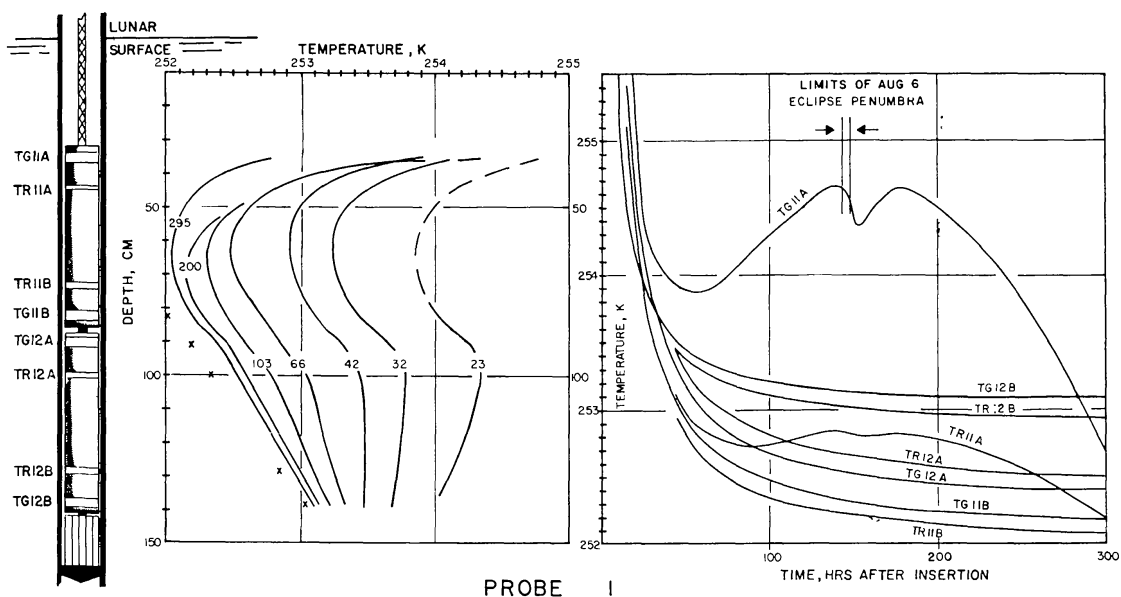


Fig. 4. Temperature histories of the sensors on probe 1 during the first 300 h after emplacement. The subsurface geometry of the probe and temperature as a function of depth are shown on the left. Temperature as a function of time is shown on the right.

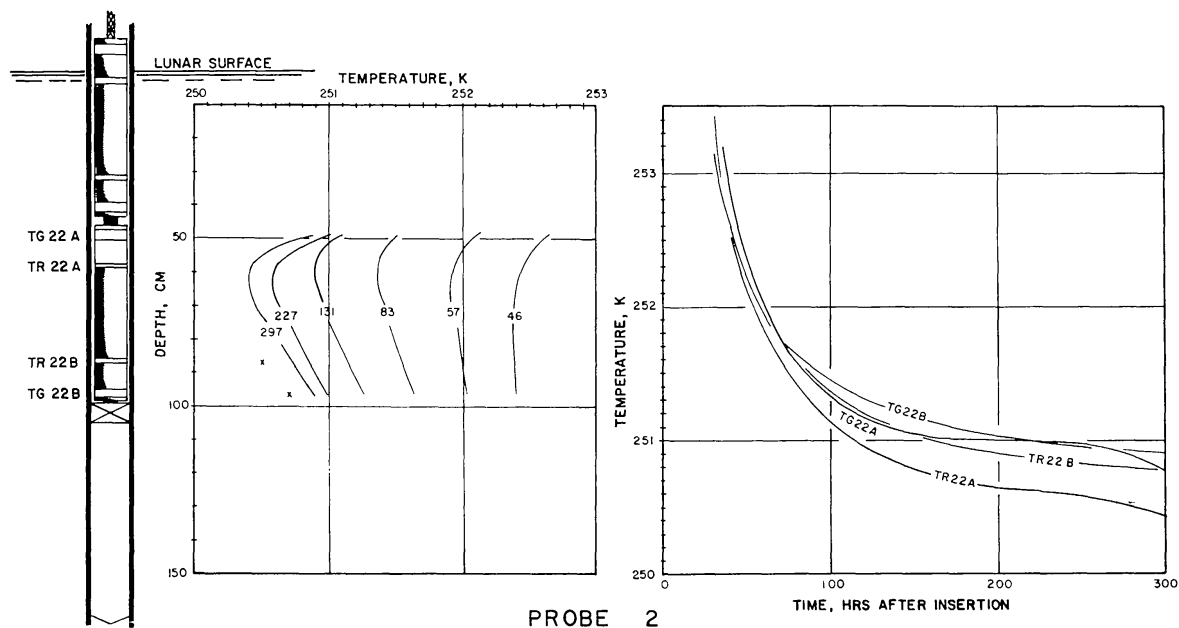


Fig. 5. Temperature histories of the sensors on probe 2 during the first 300 hr after emplacement. The subsurface geometry of the probe and temperature as a function of depth are shown on the left. Temperature as a function of time is shown on the right.

depths greater than 0.7 m continued to cool monotonically with time and were still cooling after 300 h. The thermometers at depths less than 0.7 m responded to the variations of temperatures of the borestem projecting above the surface during the lunar day. The temperature in the top of the probe 1 borestem, which is projecting above the surface, was 348 K at lunar noon. As shown in Figure 5, an obstruction prevented heat flow probe 2 from passing to the bottom of the hole; consequently, the platinum resistance thermometers in the top section are not on scale. The cool down duration of probe 2 is longer than that of probe 1, probably because of the lower conductivity material surrounding the borestem and the higher initial heat input that resulted from extended drilling.

The cool down of the probes and borestem in the regolith from their initially higher temperatures is described well by the theoretical cooling of a cylinder in an infinite medium. This theory has been extensively developed by Jaeger (1956). To analyze the temperature histories of the lunar heat flow probes, we have extended the results of Jaeger to describe a somewhat more complex case of two concentric cylinders in an infinite medium. A finite thermal resistance is assumed to exist between the two cylindrical surfaces (Langseth *et al.*, 1972).

This theory allows us to accurately extrapolate the temperature histories shown in Figures 4 and 5 to their final equilibrium temperature values. These equilibrium temperatures represent the temperatures in the regolith before the probe was emplaced. The equilibrium temperatures determined in this way are independent of the estimate of initial probe temperature.

The equilibrium temperatures for all sensors not affected by the diurnal variation, shown as  $x$ 's, are plotted as functions of depth in Figures 4 and 5. The accuracy of these equilibrium temperatures is  $\pm 0.05$  K.

At the probe 1 site, the subsurface temperature, which increases regularly with depth, is approximately 252.0 K at a depth of 80 cm. The increase along the lower 60 cm of probe 1 is approximately 1 K. For probe 2, the temperature at a depth of 80 cm is approximately 250.5 K. The two sensors on probe 2 that are unaffected by diurnal variations indicate an increase in temperature with depth at a rate comparable to the rate detected by the probe sensors. This gradient in temperature is a result of the outward flow of heat from the Moon.

## 6. Equilibrium Temperature Differences Along the Heat Flow Probes

The gradient and ring bridges enable measurement of temperature differences between points 47 cm and 28 cm apart on the probe with an accuracy of  $\pm 0.001$  K, which is far greater than the accuracy of the absolute-temperature measurements. An analysis similar to that used for the equilibration of the individual sensors can be used to extrapolate the temperature differences to equilibrium values. Only those differential thermometers that have not been affected by the diurnal variations in the first few hundred hours of observation can be used in this analysis.

The differential thermometers on the bottom section of probe 1 are the only ones



that have not been affected by diurnal variations. The calculated equilibrium temperature difference across the gradient bridge on the bottom section of probe 1 is 0.779 K and, across the ring bridge, 0.483 K. These results can be interpreted in terms of the temperature difference between adjacent points on the borestem wall by taking into account the effect of radiative coupling between the walls and the probe and the finite axial conductance of the probe. The temperature difference over the probe is always slightly less than the temperature difference between the adjacent points on the borestem. The ratio of the two, which is called the shorting ratio, was determined experimentally in the laboratory for each section of the probes. The temperature difference at points in the differential thermometers after the shorting ratio has been applied are listed in Table II.

The relatively high axial conductance of the borestem results in some axial shunting of the steady-state heat flow; therefore, to determine the undisturbed gradient (i.e., the gradient at large radial distances from the borestem), some correction must be made. The shunting effect can be estimated by modeling the borestem as a prolate spheroid

TABLE II  
Summary of equilibrium temperature difference measurements and subsurface gradients

Differential thermometer	Equilibrium temperature difference, K		Temperature gradient Moon, K/m
	Probe	Borestem	
Gradient bridge	0.779	0.819	1.74
Ring bridge	0.483	0.502	1.77

surrounded by a medium with a lower conductivity. By using an effective axial conductivity of  $2.3 \times 10^{-3}$  W/cm-K for the borestem and a lunar conductivity of  $1.7 \times 10^{-4}$  W/cm-K, the model indicates that a plus 1% correction should be applied to the borestem temperature gradients. This correction has been applied to the temperature gradients listed in Table II.

## 7. Diurnal Temperature Variations

Variations in temperature synchronous with the solar phase were observed at depths as great as 70 cm during the first one and one-half lunations after emplacement. The temperature variations measured by probes 1 and 2 are shown in Figures 6 and 7. The peak-to-peak amplitude of the variation at the top of probe 1 is approximately 6 K, a 43-to-1 attenuation of the 260 K temperature excursion measured in the part of the borestem that projects above the lunar surface. The ring sensor TR11A, which is located 9 cm below the top of the probe, measured variations with a 2 K amplitude. The sensors on the lower section of probe 2 that detected variations are somewhat deeper (49 and 58 cm) and recorded correspondingly smaller amplitudes. There are

two interesting features of the observed variations. (1) The phase shift of the peaks relative to the surface is extremely small, in view of the large attenuation factors. (2) A considerable portion of the high-frequency component of surface temperature variation penetrates to depths of 50 cm, as indicated by the rapid rates of temperature change at dawn and sunset. These features suggest that much of the heat transfer to the probe occurs by direct radiative exchange with the upper part of the borestem.

Diurnal temperature variations that propagate along the borestem have an important effect on the mean temperature in the borestem. Because the conductivity of the borestem is not as temperature dependent as the adjacent lunar material, heat will be lost more readily along the borestem at night. Consequently, the heat balance over a full lunation will require that the borestem, to depths that diurnal variations penetrate, have a lower mean temperature at a given depth than the regolith. Thus, a net cooling of the borestem can be anticipated, which is an effect that is already apparent in the substantial decrease in peak temperature during the second lunation. Comparisons with the cooling curves of deeper sensors show that this difference cannot be explained by cooling from initial temperatures alone. This cooling effect results in a gradient in mean temperature in the upper meter of the borestem that is unrelated to the heat flow from the interior.

It is essential to note that the mean temperatures and temperature differences in

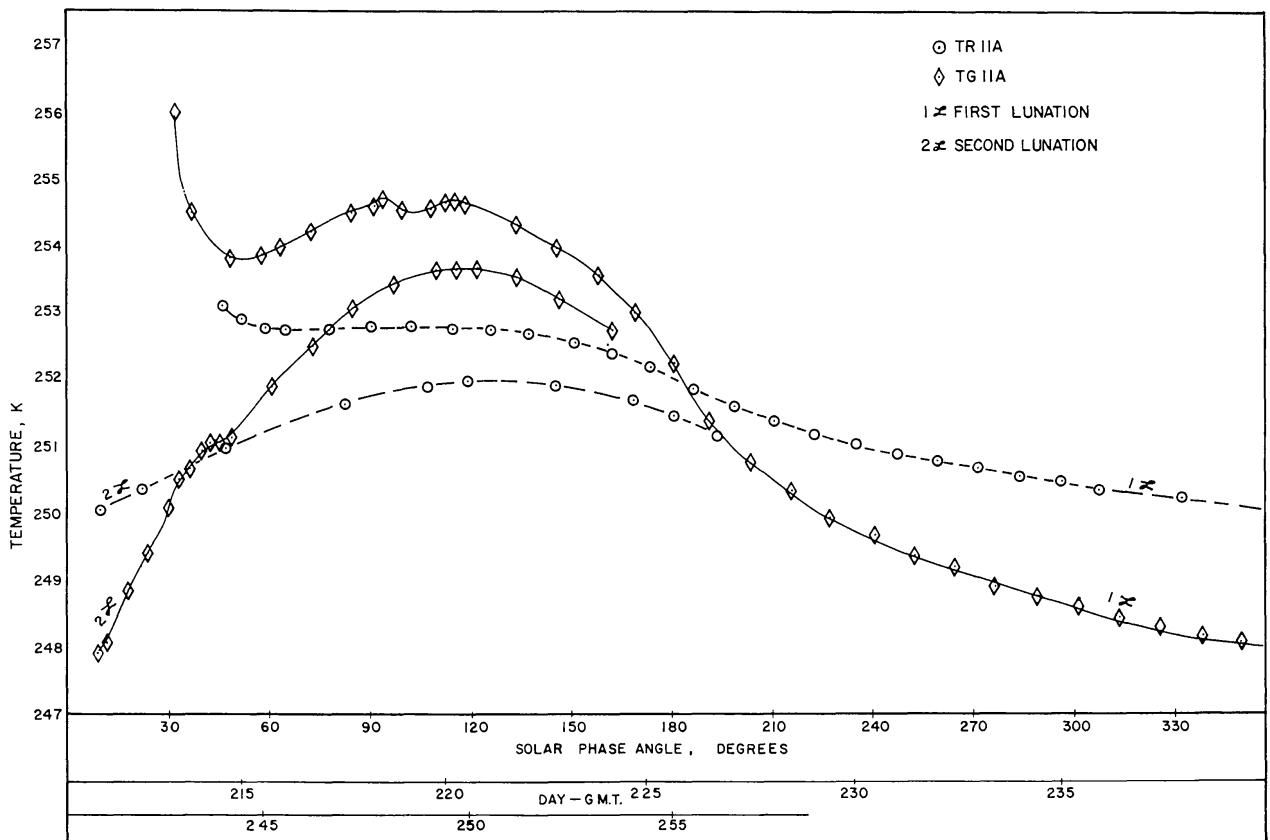


Fig. 6. Temperature as a function of solar phase angle for probe 1 sensors TR11A and TG11A for the first one and a half lunations after emplacement.

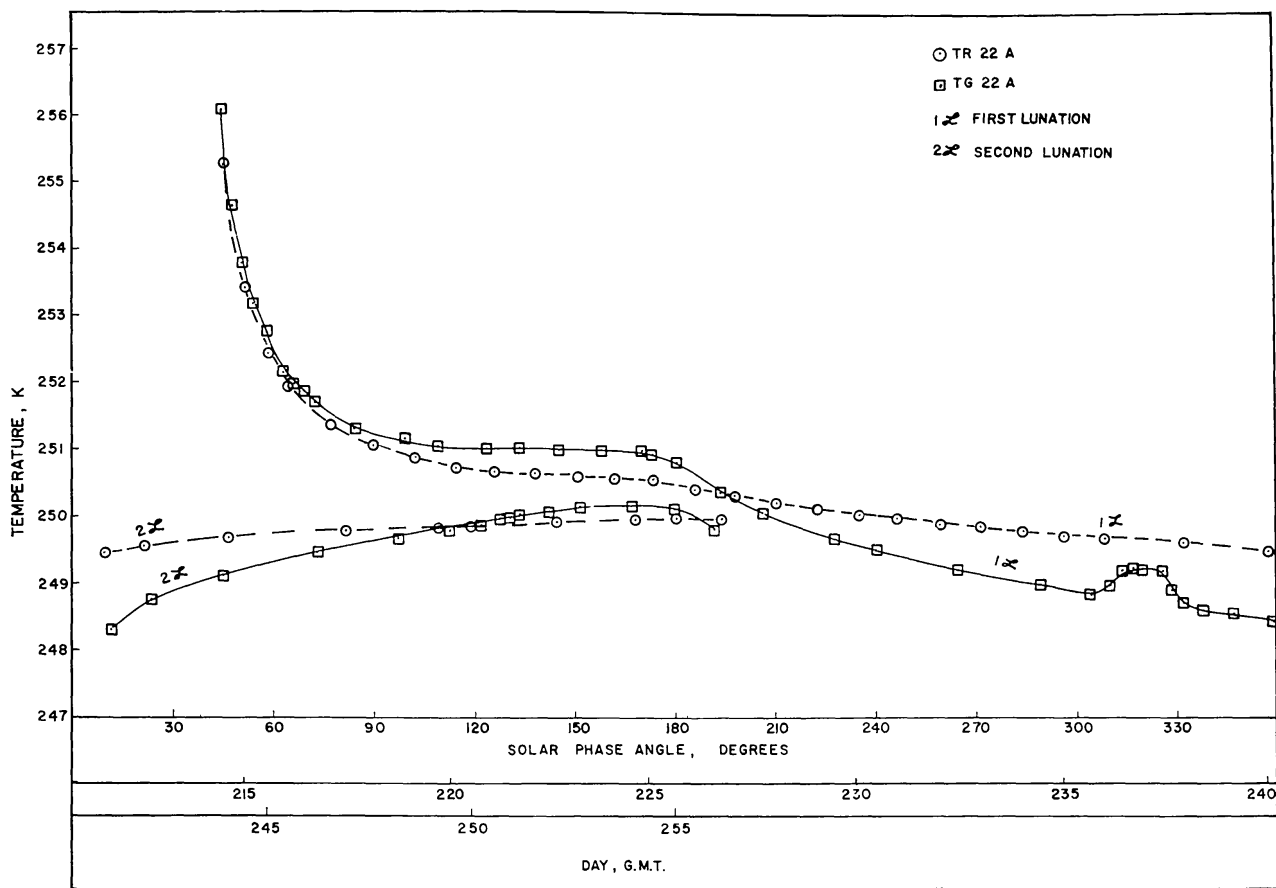


Fig. 7. Temperature as a function of solar phase angle for probe 2 sensors TR22A and TG22A for the first one and a half lunations after emplacement.

those sections of the borestem that see diurnal variations cannot be used to determine gradients related to the heat flow from the lunar interior until the effect of temperature-dependent conduction in the borestem and the surrounding lunar material is analyzed and the effect quantitatively determined. Such an analysis is beyond the scope of this preliminary report, but the analysis will be made on future subsurface temperature data after the upper part of the borestem has equilibrated nearer to the mean periodic steady-state temperature regime. This analysis will add two independent measurements of temperature gradient to the result reported here.

### 8. Implications of the Large Mean-Temperature Gradients in the Upper 50 cm at the Hadley Rille Site

By using a finite-difference model to generate daytime lunar-surface temperatures (which depend almost exclusively on the solar flux), and by using the reduced thermocouple temperatures to obtain lunation nighttime surface temperatures, a mean lunar-surface temperature of 217 K ( $\pm 3$  K) was obtained. This result indicates an increase in mean temperature (35 K higher than the mean surface temperature) at depths beyond which the diurnal variation penetrates. This phenomenon can be explained in

terms of a strong temperature dependence of the thermal conductivity, which previously has been investigated by Linsky (1966) and others. Because of the near lack of an atmosphere on the Moon, radiative transfer of heat between and through particles of the lunar fines can contribute significantly to the effective thermal conductivity. This temperature-dependent conductivity has been found to obey a relation of the form  $k(T) = k_c + k_r T^3$  (Watson, 1964), where  $k_c$  is the contribution from conduction and  $k_r T^3$  represents the radiative exchange through and between particles. Linsky (1966) has used computer models of the lunar surface to evaluate this effect in the absence of a steady-state heat flow. By interpolating from these models, the relative contributions of the conductive and radiative terms can be estimated. For a difference of 35 K in mean temperature between the surface and depths at which no significant time variations of temperature exist, the ratio of radiative to conductive terms is approximately 2 at a temperature of 350 K. The relatively small steady-state gradient (1.75 K/m) produced by the measured steady-state heat flow will have only a slight effect on this ratio. Conductivity measurements have been performed for a wide range of temperatures on returned lunar samples from the Apollo 11 and 12 missions (Cremers and Birkebak, 1972). The results also indicate the significant temperature dependence of conductivity. For Apollo 11 and 12 samples the ratios are 0.5 and 1.5, respectively. The conductivity of the more highly temperature-dependent lunar fines from the Apollo 12 site seem to be more comparable to the upper regolith conductivity at the Hadley Rille site. Further refinement of surface thermocouple data, combined with a more accurate determination of conductivity as a function of depth and direct measurements of the conductivity of returned Apollo 15 samples, will result in the first directly measured profile of regolith conductivity to a depth of 1.5 m.

## 9. Conductivity of the Regolith

### IN SITU USING-HEATERS MEASUREMENTS

Six in situ conductivity measurements in mode 2, which is the low conductivity mode, were conducted at the end of the first lunar night and during the first half of the second lunar day. The two heaters on the upper section of probe 2 were not turned on because the gradient bridges were off scale. The mode 2 measurements indicated the subsurface conductivity to be in the lower range of measurement and, in addition, showed that a substantial contact resistance exists between the borestem and the lunar material. A decision was made, therefore, not to run the mode 3 (high-conductivity mode) measurements at this time because of the possibility that the gradient sensors might reach temperatures potentially dangerous to the sensor calibration. Mode 3 measurements are planned at some future time after the effects of heater turn-on are examined by using the conductivities determined from the mode 2 results.

The interpretation of the response of the temperature-gradient sensor to heater turn-on, in terms of the lunar conductivity, is accomplished by using a detailed finite-difference model (Langseth *et al.*, 1972). A simple analytical model of the gradient-sensor long-term ( $t > 20$  hr) performance deduced from the experimental

data and the finite-difference models will be briefly discussed in the following paragraphs.

The temperature increase as a function of time at a given heater-sensor location after heater turn-on depends on the quantity of heat generated and the rate at which the generated heat can diffuse outward from the heater source. This rate will depend on the thermal properties of the material that surrounds the source. The heat will propagate axially along the probe and radially from the probe to the drill casing, across the contact-resistance layer outside the casing, and into the lunar medium. Both radiative transfer and conductive transfer are involved in the dissipation of heat. Shortly after heater turn-on, the rate of temperature increase at the gradient sensor will depend primarily on the thermal properties of the probe and the borestem in the immediate vicinity of the heater and on the resistive gaps between the probe and the borestem and between the borestem and the lunar material. As the near-sensor probe parts and borestem temperatures increase, a temperature drop is established across the resistive gaps. When this temperature difference builds to a relatively large value, heat will flow out from the borestem, across the contact-resistance gap, and into the medium; and the rate of temperature increase at the sensor will level off. At long times (times greater than 1000 min in this experiment), the temperature increase  $\Delta v(t)$ , measured at the sensor, closely fits a relation of the form

$$\Delta v(t) = C_1 \ln(t) + C_2, \quad (2)$$

where  $C_1$  and  $C_2$  are constants that depend on the contact conductances  $H_1$  and  $H_2$  and the properties of the lunar material. The finite-difference thermal model of the probe in the lunar material shows the same long-term characteristics. This relationship has the same form as the long-term solution to the problem of a uniformly heated infinite cylinder (Jaeger, 1956). As in the case of the long-term solution for a cylinder, it has been determined from the finite-difference models that, at long times after heater turn-on, the constant  $C_1$  is almost solely a function of conductivity of the surrounding material and the heat input. Thus, the slope  $[\Delta v(t_2) - \Delta v(t_1)]/\ln(t_2/t_1)$ , for times greater than 1000 min is a sensitive measure of the conductivity of the surrounding material for a constant heat input. Plots of temperature increase as a function of time for the three conductivity measurements are shown in Figure 8 and compared with best fitted theoretical models.

The magnitude of temperature increase at any time greater than 0.5 hr after heater turn-on is very sensitive to the magnitude of the contact conductance between borestem and the lunar medium. The value of the contact conductance, however, has no detectable effect on the slope of the curve of  $\Delta v$  as a function of  $\ln t$  at long times; therefore, the determination of a value for conductivity can be made independently of contact conductance by matching slopes at times greater than 1000 min. By using this value of  $k$ , a value for contact conductance was determined by varying it in the finite-difference models until the experimental curves of  $\Delta v$  as a function of  $t$  were bracketed within a small tolerance. Examples of models that bracket the experimental curves of the three in situ experiments are shown in Figure 8.

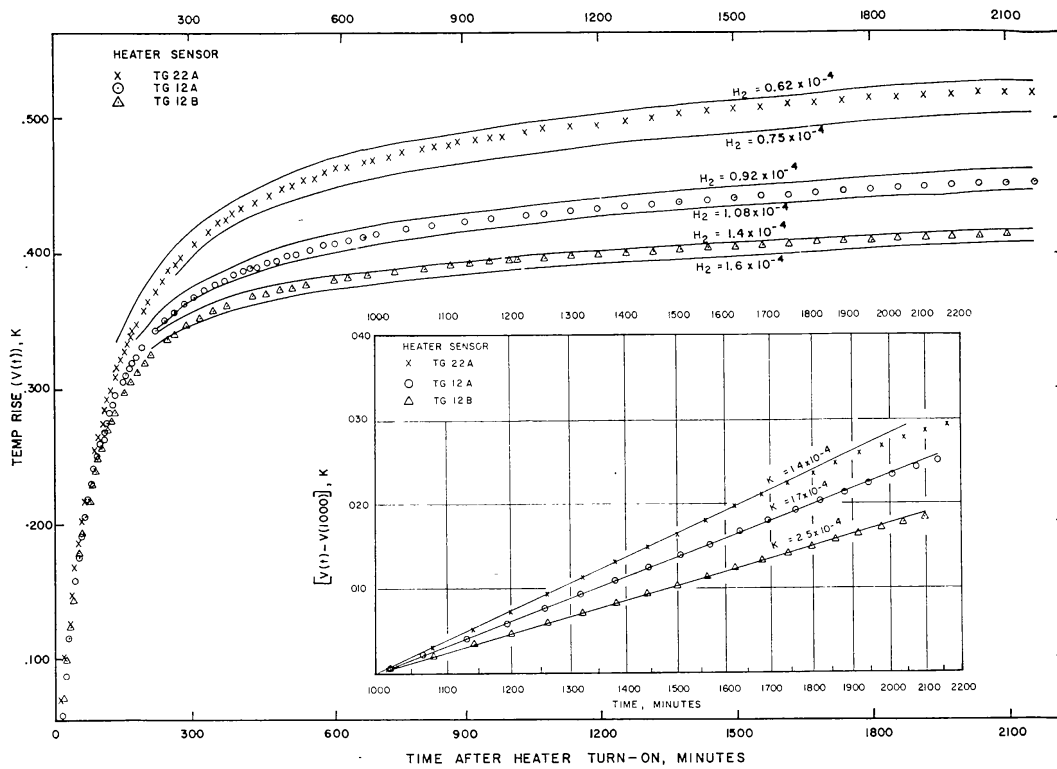


Fig. 8. Temperature increase as a function of time after heater turn-on for heaters located at sensors TG22A, TG12A, and TG12B. Two computed models that closely bracket the data are shown for each of the three heater locations. The numbers on these curves give the contact conductance,  $H_2$  in  $\text{W}/\text{cm}^2\text{-K}$ . Temperature increase as a function of time after 1000 min is shown in the inset on an expanded scale. The solid lines in the inset are best fitting computer models.  $K$ 's are the lunar conductivities used in the models.

A rather accurate determination of the conductivity of the lunar subsurface material that surrounds each heater location can be made. For example, at heater location H23 (the location of sensor TG22A), the longtime slope data could be bracketed by models of  $k = 1.3 \times 10^{-4}$  and  $k = 1.4 \times 10^{-4}$   $\text{W}/\text{cm-K}$ . A linear interpolation between these models resulted in a value  $k = 1.37 (\pm 0.02) \times 10^{-4}$   $\text{W}/\text{cm-K}$ . However, the assumption cannot be made that the models represent the physical situation this accurately; a value  $k = 1.4 (\pm 0.1) \times 10^{-4}$   $\text{W}/\text{cm-K}$  would be more realistic. Further examination of the effects of the errors introduced by the assumptions about the model parameters (probe properties, heat-transfer linkages, etc.) must be made so the error bounds of the  $k$  values can be determined. From previous limited parametric studies, a range of  $\pm 10\%$  should represent a maximum bound in the error of the  $k$ -value determinations.

The contact-conductance values determined from the in situ measurements vary. The contact conductance probably corresponds to a thin zone around the borestem that is filled with lunar fines. If the assumption is made that these fines have a conductivity of  $2 \times 10^{-5}$   $\text{W}/\text{cm-K}$ , which is similar to the conductivity of the surface fines, the widths of the disturbed zones would be 2.7, 2.0, and 1.3 mm for the locations of sensors TG22A, TG12A, and TG12B, respectively. The larger value of  $H_2$  at the

TABLE III  
Conductivity determinations from in situ experiments

Depth, (cm) (heater sensor)	$k$ (W/cm-K)	$H_2$ (W/cm <sup>2</sup> -K)
49 (TG22A)	$1.4 \times 10^{-4} \pm 0.14$	$0.7 \times 10^{-4}$
91 (TG12A)	$1.7 \times 10^{-4} \pm 0.17$	$1.0 \times 10^{-4}$
138 (TG12B)	$2.5 \times 10^{-4} \pm 0.25$	$1.5 \times 10^{-4}$

location of sensor TG12B might result from greater compaction of the fines, rather than a thinner zone. The thicker disrupted zone around probe 2 may have resulted from the longer period of drilling. The results of the conductivity measurements are summarized in Table III.

### 10. Deductions from the Heat Flow Probe Cooling Histories

The rate of equilibration of the probes depends on the thermal diffusivity  $\kappa$  of the surrounding lunar material, the ratio of heat capacity per unit volume of the lunar material to the heat capacity per unit volume of the probe, and the contact conductances between probe and borestem and borestem and lunar medium. From an analysis of the cooling history of the probes, an estimate of the diffusivity, and, thus, the conductivity of the surrounding regolith can be made.

The density of the regolith material is quite variable; preliminary measurements of samples taken by core tubes at the Hadley Rille site result in values that range from 1.35 to 1.91 g/cm<sup>3</sup>. At the depth of the probes, the densities are probably near the high end of this range and not so variable. For the analysis described in this section, a density of 1.8 g/cm<sup>3</sup> and a heat capacity of 0.66 W-s/g-K have been assumed.

It is not possible to determine a value of  $\kappa$  from the ratios of temperatures at various times during the cool down, because, as the long-term solution indicates, the temperature ratios depend solely on the ratio of the times. Bullard (1954) has pointed out this property of cooling cylinders in his discussion of sea-floor heat-flow measurements. To estimate a value for  $\kappa$ , the initial probe and borestem temperature must be known. Estimates of the initial temperature can be made by extrapolating data recorded soon after the probes were inserted to the time the borestem was emplaced. This estimate is considered to be a minimum value, because cooling during the first several minutes is faster as a result of enhanced radiative transfer at high temperatures. Alternately, the assumption can be made that the initial temperature is the temperature of the borestem before emplacement, plus some estimated temperature rise as a result of the heat produced during drilling. Temperatures recorded before emplacement by probe 2,

which was stored temporarily in the drill rack between EVA-1 and EVA-2, were used as estimates of the borestem temperature before emplacement. The temperature rise that resulted from drilling is estimated to be 15 K/min, based on estimated torque levels. The initial-temperature estimates based on these assumptions are considered to be maximum estimates.

The cooling histories of all subsurface sensors that are not affected by diurnal variations were analyzed to determine the conductivity of the surrounding lunar material

TABLE IV  
Lunar conductivities determined from probe cool down histories.

Depth	Minimum		Maximum	
	Initial temperature	Deduced conductivity	Initial temperature	Deduced conductivity
–	K	$\frac{W \times 10^{-4}}{\text{cm-K}}$	K	$\frac{W \times 10^{-4}}{\text{cm-K}}$
83 cm	315	0.8	349	1.5
87 cm	323 <sup>a</sup>	1.1	–	–
91 cm	317	1.2	349	1.7
96 cm	323 <sup>a</sup>	1.2	–	–
100 cm	317	1.2	349	1.7
129 cm	313	1.9	349	2.9
138 cm	313	2.1	349	3.3

<sup>a</sup> The borestem at probe #2 site was drilled down about 1 m on EVA I. On the second EVA, 22 hr later, the borestem was drilled an additional 3 min to a depth of about 1.5 m. The initial temperature was estimated by calculating the cool down from pre-emplacment temperature for 22 h between EVA's and adding the additional heat of drilling on the second EVA. This gave an estimate of initial temperature, 323 K, very close to that determined by extrapolation of temperature data in the first hour after insertion.

for the two limiting estimates of initial temperature. In Table IV, the maximum and minimum conductivity values determined are shown arranged in order of increasing depth. The conductivities that were determined for minimum and maximum initial-temperature estimates differ, on the average, by 50%. The more accurate conductivity measurements, which were made by using the heaters that surround the gradient sensors, resulted in values that lie within the ranges listed in Table IV. The deduced conductivity values are considerably higher than the value obtained from measurements on returned lunar fines. The value for the returned lunar fines is approximately  $2.2 \times 10^{-5}$  W/cm-K at 250 K (Cremers, 1972; Birkebak, 1972). The higher conductivity values that were obtained may be representative of fragmental regolith material in a more dense and compressed state than the surface fines.



### 11. Steady-State Heat Flow From the Lunar Interior Below the Hadley Rille Site

The conductivity of the regolith is shown by measurements to be significantly variable with depth over the lower section of probe 1. In order to compute the heat flow from temperature differences over a finite depth interval, the thermal resistance must be known. The thermal resistance can be calculated from the equation

$$R_{x_1-x_2} = \int_{x_1}^{x_2} \frac{dx}{k(x)}, \quad (3)$$

where  $x_1$  and  $x_2$  are the end points of the interval. Thus, for the flux to be determined,  $k$ -value variation in the interval between the gradient sensors, which are located at depths of 91 and 138 cm, must be known. Accurate measurements of  $k$  were made only at the end points; however, a constraint can be applied on the variation with depth from the ratio of the temperature differences measured by the ring bridge and the gradient bridge. If the heat flow is uniform with depth, the constraint required by the ratio of temperature differences is

$$\frac{\int_{100}^{129} \frac{dx}{k(x)}}{\int_{91}^{138} \frac{dx}{k(x)}} = \frac{\Delta T_{\text{ring}}}{\Delta T_{\text{gradient}}} = 0.613. \quad (4)$$

Three possible conductivity profiles were analyzed. The first, called profile *B*, is based on the trend of conductivities from the cool-down curves and obeys the constraint of Equation (4). The second (profile *A*) also obeys the constraint of equation (3) but includes a uniform conductivity of 1.7 W/cm-K to a depth of 136 cm and, then, a thin layer with a conductivity of  $2.5 \times 10^{-4}$  W/cm-K in which the bottom sensor is embedded. Profile *A* would result in a lower limit for the heat flow. The last (profile *C*) indicates a uniform increase in conductivity over the probe section. Profile *C* does not obey the constraint of Equation(3), but defines an upper limit for the heat-flow value. The trend of conductivity up to a depth of 50 cm that is indicated by the probe 2 measurement makes cases with higher conductivity than shown in profile *C* unreasonable. Based on these three profiles, the temperature difference over the lower section of probe 1 results in the heat-flow values listed in Table V. The uncertainty of the conductivity measurements ( $\pm 10\%$ ) should be considered as error bounds on each of the heat-flow values listed in Table V.

Analysis of data obtained during a full year will enable the previous determinations to be refined considerably. In addition, a comparison of the value obtained from the bottom section of probe 1 with the values obtained from the upper section of probe 1

TABLE V  
Values of heat flow based on three assumptions of  
conductivity variation with depth

Profile	Heat flow W/cm <sup>2</sup>	Comment
<i>A</i>	$2.99 \times 10^{-6}$	Lower limit
<i>B</i>	$3.31 \times 10^{-6}$	Best value
<i>C</i>	$3.59 \times 10^{-6}$	Upper limit

and the lower section of probe 2 can be made once an analysis of the effects of the diurnal variations has been completed.

## 12. Discussion of Heat Flow Results

### LOCAL TOPOGRAPHIC EFFECTS

The heat-flow determinations at the Hadley Rille site are susceptible to a number of disturbances. Corrections for some of these disturbances (such as the thermal perturbations caused by visible topographic features) can readily be made with sufficient accuracy, but other disturbances may result from refraction associated with sloping interfaces between materials of differing thermal conductivity. Such interfaces, if present at all, are hidden in the lunar interior, and only a qualitative discussion of the effects can be given.

Probe 1, the data from which were used for the preliminary determination of heat flow, is located in a small crater that has been almost filled and nearly obliterated by later bombardment. The topography associated with this old crater is so subdued that no correction for the topography is required. However, the possibility remains that the event that produced this crater also locally altered both the thickness and the physical properties of the regolith. The truth of this hypothesis cannot be verified because no observational evidence is available; however, after the data from probe 2 have been analyzed, a comparison of the two heat-flow values may provide more information.

The two most conspicuous and important topographic features near the heat-flow-experiment site are Hadley Rille and the Apennine Front. The topographic effect of the rille was calculated by fitting the rille profile with a two-dimensional Lees-type valley (cf. Birch, 1950; Jaeger and Sass, 1962). This procedure results in a correction of 4.5%, and further allowance for the Elbow, where the rille abruptly changes direction, reduces the correction to 3.5%.

A second effect of the topography around the Hadley Rille site is that the surface in the area is shaded during part of the day; consequently, the average surface temperature is lower than flat portions of the lunar surface. This local cold-spot effect has been estimated quantitatively in two ways. The radiation balance for a point halfway down the rille wall (including factors for incoming solar radiation and radiation from the opposite wall) at appropriate times of the lunar day, was calculated and used to

derive the mean temperature in the rille. Alternatively, the temperature at the vertex of the rille, which was assumed to have a symmetrical  $V$ -shape, was calculated from the solar input alone; for this geometry, the vertex sees neither wall. The temperature was assumed to vary linearly from the vertex to the top of the rille. The radiation-balance method resulted in a correction of 5 to 10%, and the vertex method resulted in a correction of 10 to 20%. The former value is considered to be the more reliable, mainly because the profile of the rille does not particularly resemble a  $V$ -shape. A correction of 10% is considered to be reasonably close to the upper limit of the effect that results from the cold rille wall.

The thermal effect of the Apennine Front was estimated in a preliminary way from the two-dimensional-slope method of Lachenbruch (1968). By assuming two-dimensional symmetry, the curves given by Lachenbruch indicate that the correction, which is negative in this case, is 10% at a maximum. Actually, the heat-flow-experiment site is in an embayment in the Apennine Front, which invalidates the two-dimensional approximation and reduces the correction. A correction of 5% would be more realistic.

In summary, the topographic effect of Hadley Rille is approximately canceled by the effect of the Apennine Front, which leaves only the cold-spot effect of the rille as a remaining correction resulting from the visible topography. This latter correction is the largest correction in any case, and seems most likely to approximate 10% of the measured heat flow.

### 13. Implications

In this section, the view was adopted that the heat flow observed at the Hadley Rille site is representative of the moonwide value, in spite of the possibilities of local and regional disturbances and large-scale variations in the lunar heat flow. Thus, the measurement is considered at face value, with full realization that future measurements may produce major changes in the conclusions. Because of the preliminary nature of the results, simple models were used. Only the linear equation of heat conduction was considered, for which the thermal diffusivity was constant.

The value that is considered to be an upper limit to the heat flow resulting from initial heat is calculated by assuming that, at the end of a convective stage in the early history of the Moon, temperatures throughout the Moon lay along the solidus for lunar basalt (Ringwood and Essene, 1971). After  $3 \times 10^9$  yr, the heat flow resulting from these very high initial temperatures is in the range of  $0.2 \times 10^{-6}$  to  $0.4 \times 10^{-6}$  W/cm<sup>2</sup>. If, as suggested by the greater ages of all known lunar rocks, partial melting throughout the Moon took place earlier, still lower values of heat flow would be associated with the initial heat. It is likely that the assumed initial temperatures are too high; however, by revising the assumed temperatures downward, the flux from the initial heat is further reduced. The initial heat contributes little to the present lunar heat flow, and the contribution can be neglected for present purposes.

The major portion of the heat flow from the Moon probably results from radioactive heat generation in the interior. It is possible to construct an infinite number of models based on nonuniform distributions of radioactivity; however, in this report,

the discussion was confined to consideration of the Moon as a sphere with uniform and constant internal heat generation. The ratio of the surface heat flow  $q$  (expressed in  $10^{-6}$  W/cm<sup>2</sup>) and the heat production  $Q$  (expressed in  $10^{-13}$  W/cm<sup>3</sup>) is shown for several times in the following list.

Time, yr	$q/Q$ , cm
$3 \times 10^9$	$3.22 \times 10^7$
4	3.58
5	3.89
infinite	5.78

With a lunar heat flow of  $3.3 \times 10^{-6}$  W/cm<sup>2</sup>, the value of  $Q$  must be in the range of  $0.57 \times 10^{-13}$  to  $1.0 \times 10^{-13}$  W/cm<sup>3</sup>. This number is far lower than the heat production of lunar basalt, which has a value of approximately  $3.5 \times 10^{-13}$  W/cm<sup>3</sup>. However, the basaltic rocks are presumably differentiates that are far more radioactive than the parent material. On the other hand, ordinary chondrite and type 1 carbonaceous chondrites generate heat at rates of approximately  $0.17 \times 10^{-13}$  and  $0.22 \times 10^{-13}$  W/cm<sup>3</sup>, respectively. The respective average rates of heat generation over the last  $4.5 \times 10^9$  yr are  $0.61 \times 10^{-13}$  and  $0.67 \times 10^{-13}$  W/cm<sup>3</sup>. Even these last figures are barely sufficient to provide the necessary flux. The conclusion is that, if the observed lunar heat flow originates from radioactivity, then the Moon must be more radioactive than the classes of meteorities that have formed the basis of Earth and Moon models in the past.

### Acknowledgements

The authors wish to express their sincere appreciation to the many individuals whose enthusiasm and efforts have made possible the successful undertaking of this experiment. In particular, we wish to thank the personnel of the five corporations that developed, fabricated, and tested the essential instrumentation: Bendix Corporation of Ann Arbor, Michigan; Arthur D. Little, Inc., of Cambridge, Massachusetts; The Data Systems Division of Gulton Industries, Inc., of Albuquerque, New Mexico; Martin-Marietta Corporation of Denver, Colorado; and Rosemount Engineering Company of Minneapolis, Minnesota. The advice, encouragement, and active support of M. Ewing and the efforts of H. Gibbon, K. Peters, and R. Perry, all of the Lamont-Doherty Geological Observatory, were essential to the success of the program. The support of G. Simmons of the NASA Manned Spacecraft Center throughout the development of the experiment is appreciated.

### References

- Baldwin, J. E.: 1961, *Monthly Notices Roy. Astron. Soc.* **122**, 513–522.  
 Birch, Francis: 1950, *Colo. Bull. GSA* **61**, 567–630.  
 Birkebak, R. C.: 1972, *The Moon* **4**, 128.

- Birkebak, R. C., Cremers, C. J., and Dawson, J.P. : 1970, *Science* **167**, 724–726.
- Bullard, E. C. : 1954, *Proc. Roy. Soc. A* **222**, 408–429.
- Cremers, C. J. : 1972, *The Moon* **4**, 88.
- Fricker, P. E., Reynolds, R. T., and Summers, A. L. : 1967, *J. Geophys. Res.* **72**, 2649–2661.
- Jaeger, J. C. and Sass, J. H. : 1962, *Geof. Pura. Appl.* **54**, 53–63.
- Jaeger, J. C. : 1956, *Austral. J. Phys.* **9**, 167–179.
- Lachenbruch, A. H. : 1968, *Rev. Geophys.* **6**, 365–400.
- Langseth, M. G., Jr., Clark, S. P. Jr., Chute, J. L., Jr., Keihm, S., and Wechsler, A. E. : 1972, 'Heat Flow Experiment', Chapt. 11, Apollo 15 Preliminary Science Report (in press).
- Langseth, M. G., Jr., Drake, E. I., and Nathanson, D. : 'Development of an In Situ Thermal Conductivity Measurement for the Lunar Heat Flow Experiment', AIAA Lunar Progress Series Volume *Lunar Thermal Characteristics* (in press).
- Lee, W. H. K. and Uyeda, S. : 1965, *Terrestrial Heat Flow*, AGU Monograph No. 8, (ed. by W. H. K. Lee), pp. 87–190.
- Linsky, J. L. : 1966, *Icarus* **5**, 606–634.
- Ringwood, A. E. and Essene, E. : 1971, *Suppl. 1, Geochem. Cosmochem.*, 769–799.
- Troitskiy, V. S. and Tikhonova, T. V. : 1970, 'Thermal Radiation from the Moon and the Physical Properties of its Upper Mantle', NASA Technical Translation NASA TT F-13, 45 from *Izvestiya vysshikh uchebnykh zavedeniy, Radiofizika*, **13**, 1273–1311.
- Watson, K. E. : 1964, 'Thermal Conductivity Measurements of Selected Silicate Powders in Vacuum from 150–350 K, II. An Interpretation of the Moon's Eclipse and Lunation Cooling Curve as Observed through the Earth's Atmosphere from 8–14  $\mu$ ', Ph.D. Thesis, California Institute of Technology, Pasadena.